

# Identification of Nutrient-Responsive Arabidopsis and Rapeseed MicroRNAs by Comprehensive Real-Time Polymerase Chain Reaction Profiling and Small RNA Sequencing[1][C][W][OA]

**Bikram Datt Pant[2], Magdalena Musialak-Lange[2], Przemyslaw Nuc[2], Patrick May[2], Anja Buhtz, Julia Kehr, Dirk Walther, and Wolf-Rüdiger Scheible***

Max-Planck Institute of Molecular Plant Physiology, 14476 Potsdam, Germany

Comprehensive expression profiles of Arabidopsis (*Arabidopsis thaliana*) *MIRNA* genes and mature microRNAs (miRs) are currently not available. We established a quantitative real-time polymerase chain reaction platform that allows rapid and sensitive quantification of 177 Arabidopsis primary miR transcripts (pri-miRs). The platform was used to detect phosphorus (P) or nitrogen (N) status-responsive pri-miR species. Several pri-miR169 species as well as pri-miR398a were found to be repressed during N limitation, whereas during P limitation, pri-miR778, pri-miR827, and pri-miR399 species were induced and pri-miR398a was repressed. The corresponding responses of the biologically active, mature miRs were confirmed using specific stem-loop reverse transcription primer quantitative polymerase chain reaction assays and small RNA sequencing. Interestingly, the latter approach also revealed high abundance of some miR star strands. Bioinformatic analysis of small RNA sequences with a modified miRDeep algorithm led to the identification of the novel P limitation-induced miR2111, which is encoded by two loci in the Arabidopsis genome. Furthermore, miR2111, miR169, a miR827-like sequence, and the abundances of several miR star strands were found to be strongly dependent on P or N status in rapeseed (*Brassica napus*) phloem sap, flagging them as candidate systemic signals. Taken together, these results reveal the existence of complex small RNA-based regulatory networks mediating plant adaptation to mineral nutrient availability.

In recent years, approximately 21-nucleotide-long microRNAs (miRs) have been recognized as important regulators of gene expression in animals and plants (Bartel, 2004; Dugas and Bartel, 2004; Kidner and Martienssen, 2005; Chuck et al., 2009). In plants, miRs were shown to posttranscriptionally regulate diverse aspects of development like leaf polarity (Emery et al., 2003), leaf shape (Palatnik et al., 2003), the transition from the juvenile to the mature growth phase (Wu and Poethig, 2006), flowering time (Aukerman and Sakai, 2003), stomatal development (Kutter et al., 2007), and nodule development (Combier et al., 2006).

MiRs also regulate the adaptation of plants to abiotic stresses, including macronutrient limitations (Sunkar and Zhu, 2004; Fujii et al., 2005; Bari et al., 2006; Chiou et al., 2006; Sunkar et al., 2007). MiR395 and miR399 have been shown to be specifically induced during sulfur and phosphorus (P) limitation, respectively (Jones-Rhoades and Bartel, 2004; Fujii et al., 2005; Bari et al., 2006; Chiou et al., 2006; Kawashima et al., 2008). MiR399 targets the transcript of an E2-conjugase that is mutated in phosphate (Pi)-accumulating Arabidopsis (*Arabidopsis thaliana*) *pho2* mutants, and this phenotype is recapitulated in miR399-overexpressing plants (Aung et al., 2006; Bari et al., 2006). MiR399 presumably acts in a dualistic manner to inhibit PHO2. It promotes transcript decay (Allen et al., 2005; Bari et al., 2006) but also appears to inhibit *PHO2* expression by repressing translation (Bari et al., 2006), a mechanism that is probably widespread in plants (Aukerman and Sakai, 2003; Brodersen et al., 2008). Recently, miR167 has been associated with lateral root outgrowth in response to nitrogen (N) limitation (Gifford et al., 2008). Primary miR transcript 167a (pri-miR167a) was shown to be approximately 5-fold repressed by N in root pericycle cells, permitting the target *ARF8* transcript to accumulate and initiate lateral root outgrowth. Furthermore, miR398 was reported to be down-regulated by oxidative stresses and copper limitation but induced by Suc, thereby repressing two copper/zinc (Cu/Zn) superoxide dismutases and a cytochrome *c* oxidase subunit (Sunkar et al., 2006; Yamasaki et al., 2007; Dugas and Bartel, 2008).

[1] This work was supported by the Max-Planck Society.

[2] These authors contributed equally to the article.

* Corresponding author; e-mail scheible@mpimp-golm.mpg.de.

The author responsible for distribution of materials integral to the findings presented in this article in accordance with the policy described in the Instructions for Authors (www.plantphysiol.org) is: Wolf-Rüdiger Scheible (scheible@mpimp-golm.mpg.de).

[C] Some figures in this article are displayed in color online but in black and white in the print edition.

[W] The online version of this article contains Web-only data.

[OA] Open Access articles can be viewed online without a subscription.

www.plantphysiol.org/cgi/doi/10.1104/pp.109.139139

Despite these examples, little information about stress- or nutrient-responsive plant miRs is available. This is due to their often low expression levels and the absence of miR or *MIRNA* gene probes on widely used transcriptomics platforms such as Affymetrix GeneChips. Custom-made microarrays can be designed to include probes for miRs and *MIRNA* genes for a broader response analysis, but these are not very sensitive (Axtell and Bartel, 2005; Liu et al., 2008). Reverse transcription followed by quantitative PCR analysis (qRT-PCR) with nonspecific double-stranded DNA-binding fluorophores, such as SYBR Green, is a powerful alternative for highly sensitive, rapid, multiparallel, and cost-effective expression analysis (Udvardi et al., 2008). Shi and Chiang (2005) and Chen et al. (2005) reported two qRT-PCR-based methods to measure the levels of mature miRs. The first approach relies on in vitro polyadenylation of mature miRs followed by RT with an oligo(dT) adapter primer and amplification using SYBR Green with a miR-specific forward primer and a compatible reverse primer. In the second approach, each specific miR is reverse transcribed from total RNA using a specific stem-loop primer, followed by TaqMan PCR amplification. Although it is desirable to quantify the biologically active mature miR species, a limitation of both qRT-PCR methods is that they are unable to differentiate the expression strengths of *MIRNA* genes that yield (nearly) identical mature miR molecules. Hence, the interpretation of the results will be dominated by strongly expressed member(s) of a given *MIRNA* gene family, while the contribution of lowly expressed members will go unnoticed. This might be especially important if these genes are expressed in an organ- or cell type-specific manner.

Deep sequencing using new technologies (e.g. Illumina-Solexa chemistry) is another approach being adopted for the analysis of small RNA/miR abundance (German et al., 2008; Moxon et al., 2008a; Szittya et al., 2008). The high number of sequence reads promises sensitivity, yet the necessary expertise required and the labor and cost involved are considerable. Data from small RNA sequencing together with miR prediction algorithms like miRDeep (Friedländer et al., 2008) also provide the basis for the discovery of novel miRs, even in organisms that have been specifically surveyed to identify miRs.

We have developed a qRT-PCR platform for parallel analysis of 177 currently known Arabidopsis *MIRNA* gene pri-miRs. This platform provides a sensitive yet inexpensive tool for Arabidopsis researchers to carry out miR expression analysis. A comparable approach has previously been described for monitoring the expression of 23 human miR precursors (Schmittgen et al., 2004). As pri-miRs are generated by RNA polymerase II in plants and animals (Bracht et al., 2004; Cai et al., 2004; Kurihara and Watanabe, 2004; Lee et al., 2004), they contain 5′ caps and 3′ poly(A) tails. The latter make the transcripts amenable to oligo (dT)-primed RT and thus multiparallel analysis by qRT-PCR. Although pri-miRs are not the biologically active molecules, several previous studies have shown that the response of a pri-miR can reflect that of the encoded mature miR (Jones-Rhoades and Bartel, 2004; Bari et al., 2006; Pant et al., 2008) and thus can serve as a valid indicator. Therefore, qRT-PCR profiling of pri-miRs can serve as a useful tool to discover responses to particular stimuli, which can then be confirmed by analysis of the mature species.

In this work, we first established the pri-miR platform and then used it to discover previously unknown nutrient-responsive pri-miRs. The corresponding mature miRs were investigated by targeted assays and further confirmed by small RNA sequencing, which also revealed novel insights. The results indicate that small RNAs play a much more important role in nutrient signaling than previously thought.

## RESULTS

### A qRT-PCR Platform for Arabidopsis pri-miRs

Sequences of 184 annotated Arabidopsis miR stem loops were obtained from the miRBase database (www.microrna.sanger.ac.uk). These sequences are not strictly pre-miRs but may include flanking sequence from the presumed pri-miR. Pri-miR sequences of members from the same family can be almost identical, complicating the design of specific PCR primers. This occurs in the miR169 family, where miR169i through miR169n are located in three highly homologous, tandem-arrayed stretches (Supplemental Fig. S1), and in the miR854 family, where the pre-miR sequences of the four annotated members are 97% to 100% identical. However, it is questionable whether miR854s are true miRs, as the sequences are located close to (or in) the centromere of chromosome 5 and are annotated as transposable elements in The Arabidopsis Information Resource (TAIR) database (www.arabidopsis.org). Therefore, we treated miR854 as a single miR, leaving a total of 181 sequences for which primers were designed.

To ensure maximum specificity and efficiency during PCR amplification of pri-miR cDNA under a standard set of reaction conditions (Fig. 1A), a stringent set of criteria was used for primer design (see "Materials and Methods"). PCR primers were tested on cDNA from Arabidopsis wild-type ecotype Columbia (Col-0) seedlings, which was free of genomic DNA contamination. Using this cDNA as template, 150 primer pairs gave unique PCR products of the expected size, while 27 primer pairs yielded no product and four gave unspecific products. The 27 primer pairs were retested using Arabidopsis Col-0 genomic DNA as template. Fifteen primer pairs resulted in the expected genomic product, showing that the primers anneal to the correct sequence and suggesting that the targeted pri-miRs (e.g. 159c, 166c, 395a to 395f, and 404; Supplemental File S2) were below the detection limit in the cDNA samples or that amplification from the cDNA

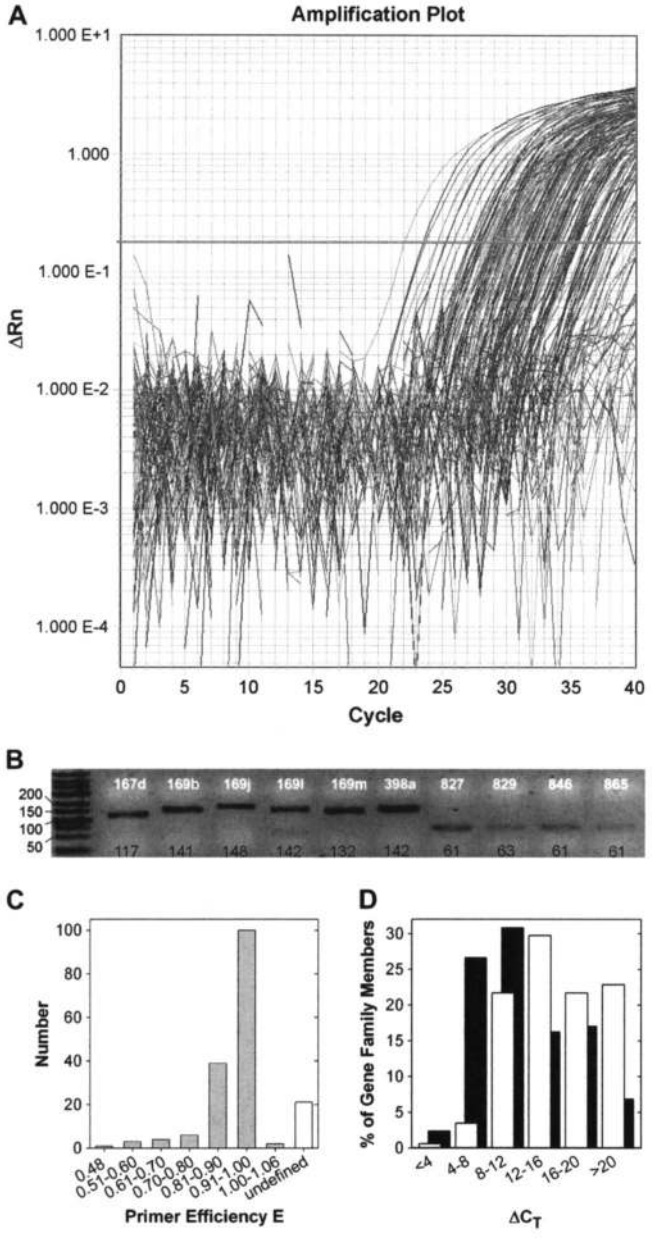


**Figure 1.** qRT-PCR platform for pri-miR transcript quantification. A, Typical real-time RT-PCR amplification plots of 175 miR amplicons showing increase in SYBR Green fluorescence (ΔRn; log scale) with PCR cycle number. Note the similar slope of most curves as they cross the fluorescence threshold of 0.18 (green line), which reflects similar amplification efficiency. B, Separation of PCR products on 4% (w/v) high-resolution agarose gels reveals single products of the expected size (black numbers). A selection of 10 amplicons is shown. Size standards in bp are indicated to the left. C, Distribution of efficiencies for 154 primer pairs (gray bars). For 21 primer pairs (white bar) no primer efficiencies were obtained in the conditions investigated. D, Expression strength distribution of *MIRNA* genes (white bars) and of transcription factor genes (black bars). Genes were grouped according to their $\Delta C_T$ values, calculated with UBQ10 as reference. [See online article for color version of this figure.]

was inhibited. Evidence in support of the former hypothesis comes from the observation that some of the primers (e.g. pri-miR395a to -395f) did amplify the expected products from a cDNA sample derived from sulfur-limited seedlings (Supplemental Fig. S2). The 16 primer pairs that did not yield any product from cDNA or genomic DNA templates, or that amplified unexpected/unspecific products, were redesigned, finally resulting in 175 validated primer pairs and only six *MIRNA* genes (highlighted in red in Supplemental File S2) for which no working pairs could be established.

Specificity of PCR primers was assessed by melting curve analysis of PCR products (Supplemental Fig. S3), by separating the PCR products via electrophoresis on high-resolution agarose gels (Fig. 1B), and by double-stranded sequencing of a subset of the pri-miR PCR products (Supplemental Fig. S4). In all cases, the sequences of the PCR products were identical to those of the intended pri-miR targets. The average amplification efficiency (E) of the primers, as determined by LinRegPCR (Ramakers et al., 2003), was high; for 102 primer pairs, E was greater than 90%, and for another 39 pairs, E was 81% to 90% (Fig. 1C; Supplemental File S2). Twenty-one primer pairs did amplify a correct product from genomic DNA, but no product was obtained with cDNA from the samples investigated (see below); hence, no E value could be established for these primers.

The fraction of pri-miRs detected (i.e. expressed in at least two biological replicates with a threshold fluorescence cycle number [$C_T$] of less than 40) was just below 80%, irrespective of the growth conditions tested (Supplemental File S2). This percentage is comparable to the percentage of transcription factor (TF) genes detected at this threshold (approximately 83%; Czechowski et al., 2004). However, the average $\Delta C_T$ value of pri-miRs was higher than for the TF gene transcripts (Fig. 1D). Hence, pri-miRs are often less abundant than TF transcripts. Low abundance ($C_T$ > 33) also resulted in higher variability between replicate measurements, making detection of small expression changes less reliable.

### Identification of N- and P-Responsive Arabidopsis pri-miRs

The qRT-PCR platform was used to identify pri-miRs that are induced or repressed in 9-d-old Arabidopsis seedlings during N or P limitation (Supplemental File S2). The expected physiological status of the seedlings was confirmed by evaluation of marker gene expression (Supplemental Fig. S5). *NRT2.5* (*At1g12940*) and *AMT1.5* (*At3g24290*) were both strongly induced in N-limited seedlings, and *PHT1.4* (*At2g38940*) was induced by P limitation, as found previously (Scheible et al., 2004; Morcuende et al., 2007).

Twenty pri-miRs exhibited differential expression in N- or P-limited conditions (Fig. 2), based on an average change in normalized cycle number of at least three ($|\Delta\Delta C_T| \geq 3$) between nutrient limitation and

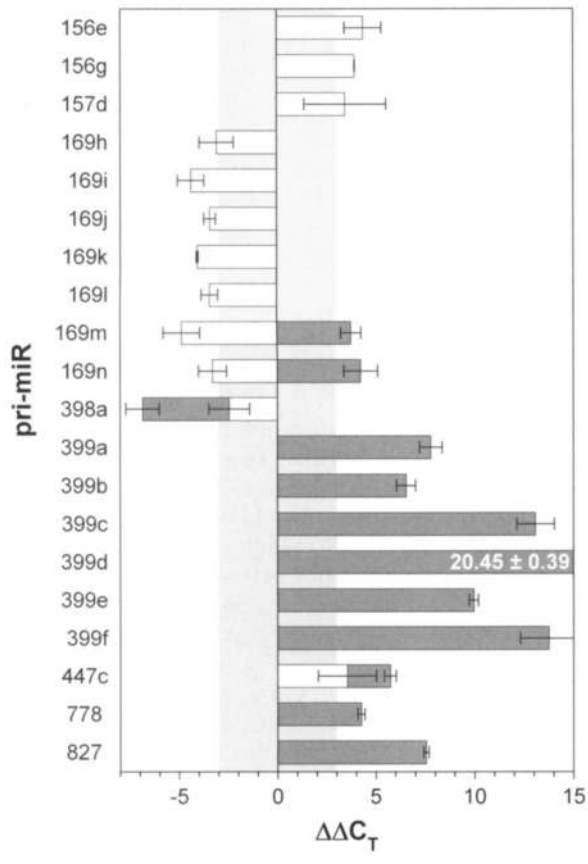


**Figure 2.** Identification of N/P limitation-responsive pri-miRs in Arabidopsis. For each pri-miR species, the average $\Delta\Delta C_T$ value ± SE from three biological replicates (with two technical replicates for each) is depicted. $\Delta\Delta C_T = \Delta C_{T\,FN} - \Delta C_{T\text{-}nutrient}$, and $\Delta C_T = C_{T\,pri\text{-}miR} - C_{T\,UBQ10}$. Pri-miRs induced in nutrient limitation thus have a positive $\Delta\Delta C_T$ value and vice versa. The fold induction can be inferred from the equation $(1 + E)^{\Delta\Delta C_T}$, where E is PCR efficiency (Supplemental File S2). Only pri-miRs with average $\Delta\Delta C_T$ values of >3 or <−3 (as indicated by the light gray shading) are shown. Results for P and N limitation are shown as dark gray and white bars, respectively.

full nutrition (FN). The most prominent change was the known induction of pri-miR399s during P limitation, with $\Delta\Delta C_T$ ranging from 6.5 to 20 (Fig. 2; Bari et al., 2006). Pri-miR399d was undetectable in FN conditions and rose to levels comparable to some of the most strongly expressed genes in Arabidopsis, such as *UBQ10* (Czechowski et al., 2005). Very high expression of pri-miR399s and mature miR399 during P limitation is necessary to fully suppress the activity of its target *PHO2* transcript (Bari et al., 2006). Mechanistically, this seems to involve translational repression, as suggested by previous results (Bari et al., 2006) and our finding that miR399d-overexpressing seedlings have substantially lower but still detectable levels of *PHO2* transcript (10%–20% of control plants), while their molecular phenotypes are identical to *pho2* seedlings (Supplemental Fig. S6).

qRT-PCR profiling revealed several pri-miR species for which nutrient responsiveness was previously unknown: pri-miR447c, -778, and -827 all increased ($\Delta\Delta C_T$ = 4.2–7.6) during P starvation, whereas pri-miR398a strongly decreased ($\Delta\Delta C_T$ = −6.9; Fig. 2; Supplemental File S2). Also, pri-miRs 169m and 169n displayed induction ($\Delta\Delta C_T$ = 3.7–4.2) during P limitation, and the same two pri-miR169s plus five additional ones (pri-miR169h through -169l) were decreased ($\Delta\Delta C_T$ = −3.1 to −4.9) in N-limited seedlings (Fig. 2).

Pri-miR398a and pri-miR447c were not only responsive to P limitation but also showed similar responses in N limitation, albeit not as strong, with pri-miR398a being slightly repressed ($\Delta\Delta C_T$ = −2.45; Supplemental File S2) and pri-miR447c induced ($\Delta\Delta C_T$ = 3.5; Fig. 2). Furthermore, pri-miRs156e, -156g, and -157d were found to be induced ($\Delta\Delta C_T$ = 3.1–4.4) in N-limited seedlings. Pri-miR167a, which was reported to be more highly expressed in N-limited root pericycle cells (Gifford et al., 2008), showed no clear response in our experiments with N-limited seedlings. However, pri-miR167d was less expressed ($\Delta\Delta C_T$ = −2.5) in N-limited seedlings (Supplemental File S2).

### Nutrient-Responsive Mature miR Species

To examine if the mature miRs derived from the nutrient-responsive pri-miRs also showed a nutrient response, we used a qRT-PCR approach similar to the one described by Chen et al. (2005; Supplemental Table S1). In addition to nutrient-replete (FN), N-limited (−N), and P-limited (−P) Arabidopsis seedlings, we also included carbohydrate-limited (−C) seedlings (Supplemental Fig. S5) in the analysis. Mature miR399s were not analyzed, since their high abundance during P limitation is already well documented (see introduction).

MiR778 and miR827 were both strongly induced by P limitation, thus confirming the response of their pri-miRs. However, they did not respond to either N or C limitation (Fig. 3) and remained almost undetectable under these conditions, suggesting that both of these miRs are involved in P-specific regulation events. The response of miR398a was also similar to that of the corresponding pri-miR, being decreased by P and N limitation and also by C limitation (Fig. 3).

Given the previous report of Gifford et al. (2008) and the moderate repression of pri-miR167d we observed in N-limited seedlings, we also investigated miR167. The assay for miR167 showed a relatively high expression level ($40 - \Delta C_T = 35$), but this might be due to low specificity in the assay leading to detection of miR167 derived from several primary transcripts. Our result obtained with N-limited seedlings (Fig. 3) does not confirm the reported down-regulation of miR167 in root pericycle cells by organic N (Gifford et al., 2008). Possible explanations for this discrepancy are the nonspecificity of the assay for miR167 and/or the lack of spatial resolution in our analysis, which could mask any cell type-specific response of a particular *MIRNA* gene and its derived miR.

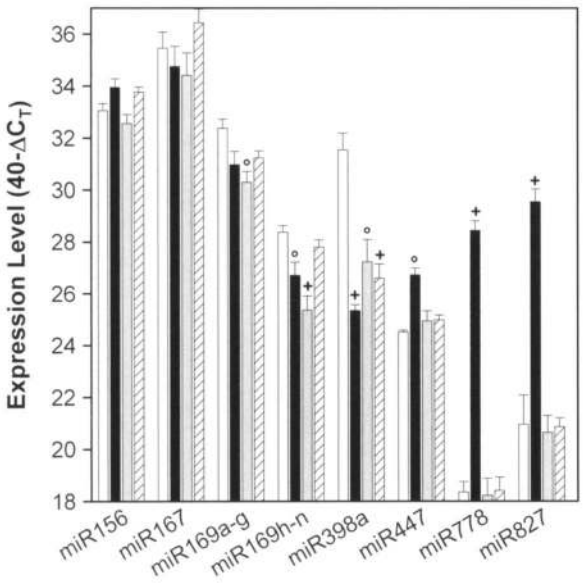


**Figure 3.** Nutrient responsiveness of mature miRs. qRT-PCR results are shown for nutrient-replete (white bars), P-limited (black bars), N-limited (gray bars), and C-limited (hatched bars) Arabidopsis seedlings. Expression levels are given on a logarithmic scale expressed as 40 − $\Delta C_T$, where $\Delta C_T$ is the difference in qRT-PCR threshold cycle number of the respective miR and the reference gene *UBQ10* (*At4g05320*); therefore, 40 equals the expression level of *UBQ10* (the number 40 was chosen because the PCR run stops after 40 cycles). The results are averages ± SE of three biological replicates. Significance of the changes found during P, N, or C limitation was checked with Student's *t* test. $P < 0.05$ is indicated by circles, and $P < 0.01$ is indicated by plus signs.

Nucleolytic cleavage of pri-miR169h to -n (Supplemental Fig. S1) by the DICER endoribonuclease results in identical miR169 molecules, precluding a specific assay. Nonetheless, since all seven pri-miR sequences were less abundant in N limitation (Fig. 2), we were able to confirm lower miR169h to -n levels in N limitation (Fig. 3). The moderate induction found for two of these pri-miR169 species during P limitation was not supported by the miR169h to -n assay; on the contrary, mature miR169h to -n showed a significant (approximately 3-fold) decrease in P limitation. A second assay designed for miR169a to -g also indicated lower abundance during N and P limitation (Fig. 3), although no clear change was detected for the corresponding pri-miRs.

We were also able to confirm a slight induction ($\Delta\Delta C_T \sim 2$) of miR447 during P but not N limitation, whereas the induction of miR156 during N limitation, as suggested by pri-miR156e and -156g (Fig. 2), was not confirmed (Fig. 3). Again, a nonspecific assay and high expression of other pri-miRs from the same family (Supplemental File S2) probably account for this discrepancy.

### P Status-Responsive miRs Detected by Small RNA Sequencing

As an independent approach to verify the P responsiveness of mature miRs, we used small RNA sequencing (SRS) with Illumina-Solexa technology. Three cDNA libraries prepared from nutrient-replete (FN) seedlings, P-limited (−P) seedlings, and −P seedlings that were resupplied with 3 mM phosphate for 3 h were sequenced (Supplemental Table S2). Sequence reads with 100% identity to Arabidopsis pre-miRs were extracted, and identical reads were totaled (Supplemental Table S2; Supplemental Fig. S7; Supplemental File S3) and normalized for each library. A plot of the distribution of read lengths for pre-miR-matching sequences (Supplemental Fig. S7A) illustrates that these consist almost exclusively of 20- and 21-mers, with the latter being the most abundant, whereas a plot of all genome-matching sequences reveals a substantial number of 24-mers and other lengths (Supplemental Fig. S7B). Comparison also shows a significantly (approximately 30%) higher number of 21-mers in the group of genome-matching sequences, possibly indicating the presence of unknown miRs.

The normalized read numbers for miR399s were high during P limitation and very low in nutrient-replete (FN) conditions (Fig. 4A), as expected (Bari et al., 2006; Pant et al., 2008). There was no appreciable decrease of miR399s at 3 h after Pi readdition, supporting earlier results that suggested that miR399s are rather stable (Bari et al., 2006). SRS also confirmed high expression of miR778 and miR827 during P limitation (Fig. 4A). Very few (one or two) or no reads were obtained for miR398a, -447c, -845, or -169h to -n, whereas these miRs were detectable by qRT-PCR, suggesting that our qRT-PCR analysis was more sensitive than the SRS approach. SRS showed three additional miRs (i.e. miR408, miR829, and miR863) to be 4- to 10-fold more abundant during P limitation. Analysis by qRT-PCR supported the increase in levels of miR408 but was unable to confirm the higher abundance of miR829 or miR863 (Supplemental Fig. S8).

Surprisingly, sequence reads representing star (*) strands of some of the nutrient-responsive miRs (i.e. miR398a*, miR399a*, miR399c*, miR399d*, miR399f*, and miR778*) were found to be present in numbers similar to, or exceeding (up to 200-fold in the case of miR398a*), those for the corresponding miRs (Fig. 4A; Supplemental File S3), whereas others (e.g. miR399b*, miR827*, and miR863*) were absent. The presence of star strands and their specific induction by Pi limitation was confirmed by qRT-PCR (Supplemental Fig. S8). These results raise the question of the biological function of these abundant miR*s. Another interesting observation from the SRS was that the sequence reads corresponding to miR778 and miR863 do not perfectly agree with the annotated miR sequences determined from flower samples (Fahlgren et al., 2007) but look to be shifted by one or several nucleotides (Supplemental File S3). Furthermore, the miR778/miR778* duplex appears to be unusual in having a 5′ overhang that is seven nucleotides long (Supplemental File S3). These results from Arabidopsis seedlings could indicate that the cleavage site of some pre-miRs by DICER proteins

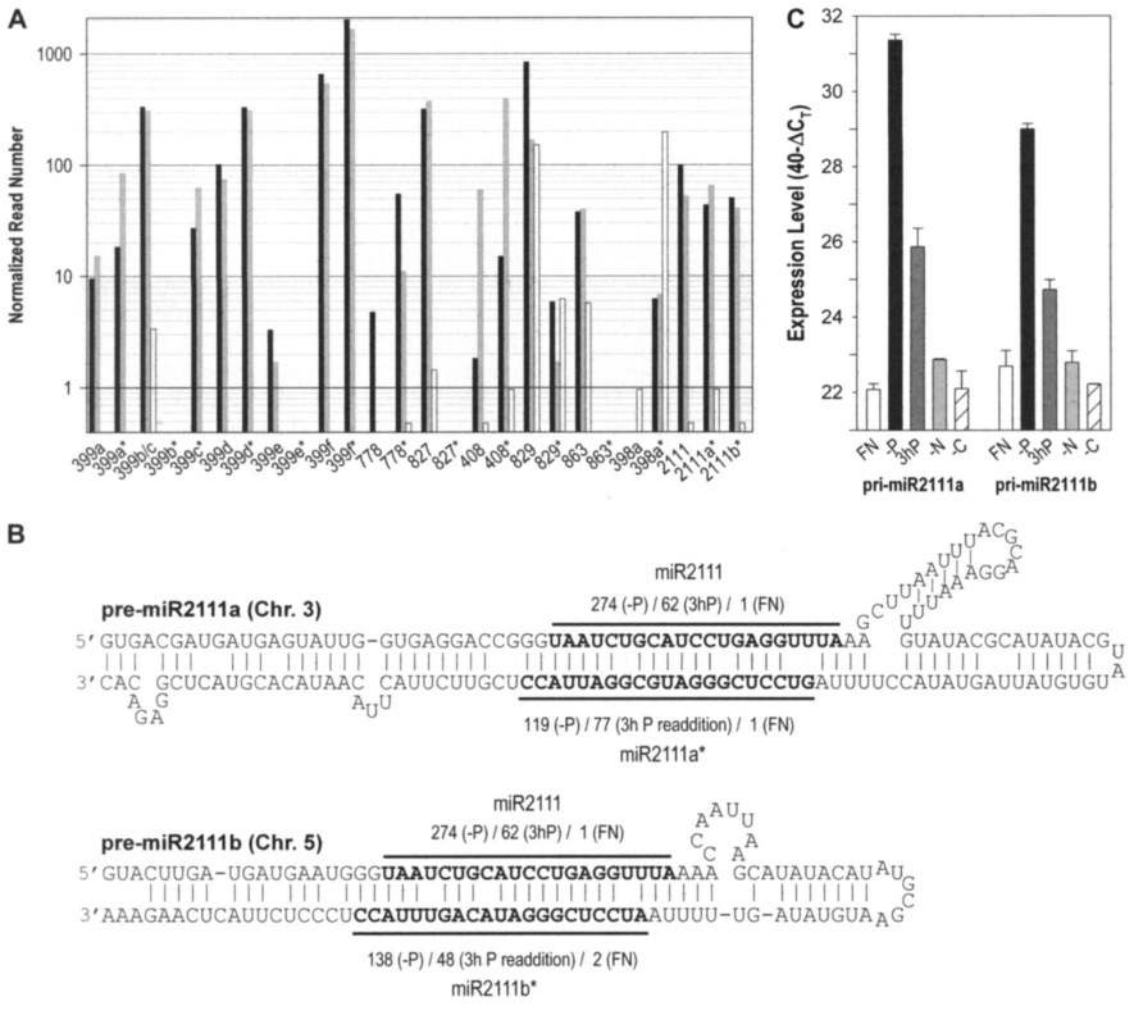


**Figure 4.** P-responsive miRs as detected by small RNA sequencing. A, The number of normalized sequence reads (ppm) is shown for all miRs and their corresponding star (*) strands that show at least a 5-fold change between P limitation (black bars) and P-replete (white bars) conditions and for which at least 10 total reads were scored in at least one condition (Supplemental File S3). Normalized read numbers are also shown for a time point of 3 h after resupply of 3 mM potassium phosphate to previously P-limited seedlings (3hP; gray bars). Missing bars indicate zero reads. B, Putative miR2111a and -b precursor sequences and structures. The sequences of mature miR2111 and the presumed star strands are shown in boldface on the top and bottom strands, respectively. The number of absolute reads for the three conditions tested (see A) is indicated. C, qRT-PCR expression of the 82- and 103-nucleotide-long pri-miR2111a and -b amplicons in various conditions (FN, full nutrients; −P, P limitation; 3hP, 3 h of Pi readdition; −N, N limitation; −C, carbohydrate limitation). Expression levels are plotted on a logarithmic scale as described in the legend to Figure 3. The results are averages ± SE of three biological replicates with two technical replicates for each.

is not totally fixed and may change with developmental stage.

### Discovery of a Novel P Status-Responsive miR

The SRS data were analyzed further to look for novel P status-dependent miRs. Candidate miRs were predicted using a miRDeep algorithm (Friedländer et al., 2008) that was adapted for plant miR precursor sequences (P. May and M. Friedländer, unpublished data). Among the predicted miR candidates was one, named miR2111, that showed a very strong dependence on P status (Fig. 4A). It is highly abundant during P limitation but almost absent in nutrient-replete seedlings and so closely resembles the behavior of known P-responsive miRs (miR399s, miR778, and miR827) in these conditions. When Pi is resupplied to Pi-limited seedlings, the abundance of the novel miR2111 fell by approximately 2-fold within 3 h of Pi readdition (Fig. 4A). This response differs from those of miR399s and miR827, which do not fall rapidly after Pi readdition, but is similar to that of miR778, suggesting that the biological half-lives of miRs can vary considerably.

The DNA sequence of miR2111 is present twice in the Arabidopsis genome: upstream of *At5g02040*, and between *At3g09280* and *At3g09290*. For these locations, the algorithms miRDeep and miRCat (http://srna-tools.cmp.uea.ac.uk) predicted two precursor sequences/structures, named pre-miR2111a and -b (Fig. 4B). The observation that the read numbers of the two star strands (miR2111a* and miR2111b*) are similar and that they decrease after Pi readdition or are almost absent in P-replete conditions reveals that both loci have P-responsive expression and contribute to a similar extent. The strong P limitation response of miR2111 was confirmed by qRT-PCR (Supplemental Fig. S8). In addition, PCR products designed to encompass larger stretches (82 and 103 nucleotides) of pre-miR2111a and -b could be amplified from oligo (dT)-primed cDNA pools, showing that miR2111 is derived from poly(A)-tailed primary transcripts, and these also displayed strong P responsiveness (Fig. 4C). Furthermore, both the mature miR2111 and its pri-miRs displayed specificity for P, as N or C limitation did not affect the expression levels (Fig. 4C; Supplemental Fig. S8). We were also able to find potential orthologs of pre-miR2111s in rapeseed (*Brassica napus*; Supplemental Fig. S9). The rapeseed 2111a and 2111b precursors share 85% and 83% identity at the DNA level with their Arabidopsis counterparts and are predicted to fold into stable extended hairpin structures by the miRCat algorithm. PCR primer pairs for Arabidopsis pri-miR2111a and -2111b were added to the qRT-PCR platform, thus bringing the number of *MIRNA* genes represented to 177 (Supplemental File S2).

### MiRs with P or N Status-Dependent Abundance in Rapeseed Phloem Sap

MiR399 was previously found to be highly abundant in phloem sap from rapeseed and pumpkin (*Cucurbita maxima*) during P limitation and to constitute a shoot-derived long-distance signal for the regulation of plant Pi homeostasis (Buhtz et al., 2008; Lin et al., 2008; Pant et al., 2008). To test whether additional miRs show nutrient status-dependent abundance in phloem sap, we collected sap from nutrient-replete, P-limited, and N-limited rapeseed plants and prepared small RNA libraries for sequencing.

Analysis of the resulting small RNA reads (Supplemental Table S3) showed that sequences homologous to miRs known to be present in the phloem (e.g. miR156, miR159, and miR167) were present in the libraries, whereas sequences homologous to miR171, which is abundant in leaf or stem tissue but undetectable in phloem (Yoo et al., 2004; Buhtz et al., 2008), were completely absent (Fig. 5A). This indicates that the phloem sap samples were not noticeably contaminated with small RNAs from stem tissue. Small RNA species found in the libraries should thus represent authentic phloem constituents. The high purity of rapeseed phloem sap obtained using the same method was previously reported by Giavalisco et al. (2006) and Buhtz et al. (2008).

Further analysis revealed that in addition to Bna-miR399 (Fig. 5B; Pant et al., 2008), a Bna-miR399-like sequence, Bna-miR2111, a Bna-miR2111-like sequence, and an Ath-miR827-like sequence are highly abundant in rapeseed phloem sap during P limitation, while no sequences homologous to the P-responsive Ath-miR778 were found. We were also able to determine that (1) two sequences with homology to Ath-miR399d* and Ath-miR399f*, (2) Bna-miR2111a* and Bna-miR2111b*, and (3) five miR2111*-like sequences were clearly present in phloem sap during P limitation but absent or much less abundant in phloem sap of nutrient-replete or N-limited rapeseed (Fig. 5B). Furthermore, we found Bna-miR169m to be present in phloem sap of nutrient-replete plants, and the relative abundance of this species strongly decreased in phloem sap of N-limited or P-limited rapeseed plants (Fig. 5B). These results pinpoint miR2111s, miR2111*s, miR399*s, miR827, and miR169 as novel candidate long-distance signals for reporting P or N status in the plant system and suggest an expansion of the miR2111 family in rapeseed.

### Target Predictions for Nutrient-Regulated miRs

To identify candidate miR target genes, we used four prediction algorithms: miRU (Zhang, 2005), target search in WMD2 (Ossowski et al., 2008), the prediction tool in the UEA plant sRNA toolkit (Moxon et al., 2008b), and PITA (Kertesz et al., 2007). In addition, we mined experimental data from degradome studies (Addo-Quaye et al., 2008; German et al., 2008). The first three algorithms score the complementarity of miR and target RNA sequences based on established rules (e.g. the "seed rule"; Allen et al., 2005), thereby also exploring the observation that plant miRs seem to bind almost perfectly to their cognate mRNAs (Rhoades et al., 2002; Lai, 2004). In contrast, PITA assesses site accessibility in miR target recognition. This includes prediction of target RNA secondary structure and calculation of the free energy gained from the formation of the miR-target duplex and the energetic cost of unpairing the target to make it accessible to the miR. All candidate miR targets predicted with miRU, WMD2, or the UEA plant sRNA toolkit, and up to 20 best targets from the PITA analysis, are shown in Supplemental File S4, with a selection of the predicted targets shown in Table I.

In addition to the confirmed miR399 target *PHO2*, a potential target of miR399b/c predicted by all algorithms is the receptor kinase gene *ACR4*, which restricts formative cell divisions in the Arabidopsis root (De Smet et al., 2008). Another repeatedly predicted miR399b/c target is *At4g00170*, encoding a vesicle-associated membrane protein. A DEAD box helicase gene (*At4g09730*) appears as a candidate miR399a/d target from analysis with conventional prediction algorithms, whereas PITA analysis identifies *IPS1*, a

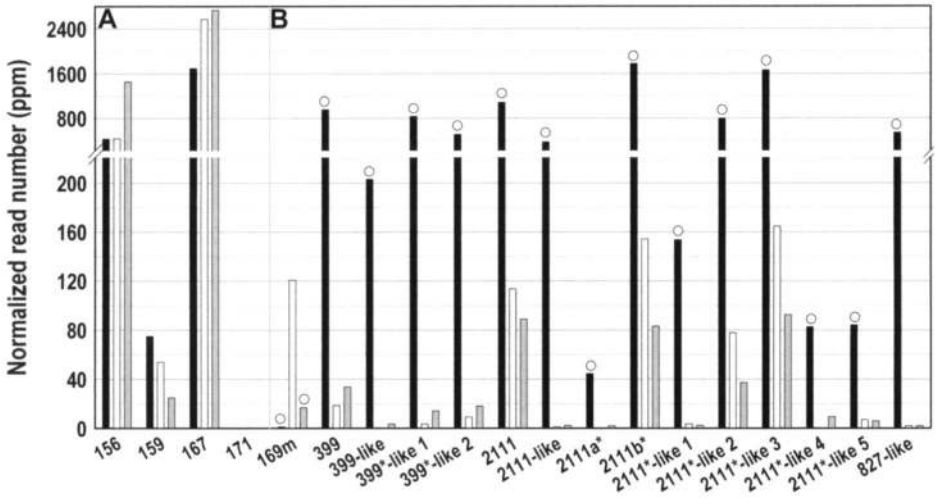


**Figure 5.** miRs with P or N status-dependent abundance in rapeseed phloem sap. A, Abundance of miRs known to be present (miR156, miR159, and miR167) or absent (miR171) in rapeseed phloem sap. B, MiR and miR* sequences with P or N status-dependent abundance. Depicted are normalized read numbers as detected by Solexa sequencing in small RNA libraries prepared from phloem sap samples of P-starved (black bars), nutrient-replete (white bars), and N-starved (gray bars) rapeseed plants. The significance of the changes between P-starved (or N-starved) and nutrient-replete conditions was analyzed with a $\chi^2$ test and Benjamini-Hochberg *P* value correction; $P < 0.0003$ is marked with circles. Sequences of the species shown are as follows: 169m, 5′-TGAGCCAAAGATGACTTGCCG-3′; 399, 5′-TGCCAAAGGAGATTTGCCCGG-3′; 399-like, 5′-TGCCAAAGGAGATTTGTCCGG-3′; 399*-like 1, 5′-GGGCGAATACTCTTATGGCAGA-3′; 399*-like 2, 5′-GGGCAAGATCTCTATTGGCAGA-3′; 2111, 5′-TAATCTGCATCCTGAGGTTTA-3′; 2111-like, 5′-TAATCGGCATCCTGAGGTTTA-3′; 2111a*, 5′-ATCCTCGGGATACAGATTACC-3′; 2111b*, 5′-GTCCTCGGGATGCGGATTACC-3′; 2111*-like 1, 5′-ATCCTCGGGATGCGGATTACC-3′; 2111*-like 2, 5′-ATCCTCGGGATACGGATTACC-3′; 2111*-like 3, 5′-ATCCTCGGGACACAGATTACC-3′; 2111*-like 4, 5′-GACCTCAGGATGCGGATTACC-3′; 2111*-like 5, 5′-TCCTCGGGATACAGATTACC-3′; 156, 5′-TGACAGAAGAGAGTGAGCAC-3′; 159, 5′-TTTGGATTGAAGGGAGCTCTA-3′; 167, 5′-TGAAGCTGCCAGCATGATCTA-3′; 171, 5′-TGATTGAGCCGCGCCAATATC-3′.

miR399 target-like interactor (Franco-Zorrilla et al., 2007). There are also clear target predictions for miR399*s, with *At3g11130*, encoding a clathrin heavy chain and thus another protein involved in vesicle transport in the secretory pathway, being a potential target of miR399d*. One of the best potential targets of miR399f* is the *CLAVATA3*-related *At3g25905/CLE27*, a gene encoding a small peptide that is highly expressed in shoot apices (Sharma et al., 2003).

Obvious targets of miR827 are the E3 ligase gene *NLA* (*At1g02860*) and its homolog *At1g63010* (Table I; Fahlgren et al., 2007). Also, miR2111 is predicted to target an E3 ligase gene (*At3g27150*) and a calcineurin-like phosphoesterase gene (*At1g07010*). A likely target of miR778 is the histone methyltransferase gene *SUVH6* (*At2g22740*), with *SUVH5* (*At2g35160*) being a possible target as well. Interestingly, miR2111a* and miR2111b* also appear to target genes required for chromatin remodeling/modification (i.e. *At2g23380/CURLY LEAF* and *At2g28290/SPLAYED*).

Confirmed targets of miR398a include two Cu/Zn superoxide dismutase genes (*CSD1* and *CSD2*) and *COX5b.1* (see introduction). The prediction algorithms detected *CSD1*, *COX5b.1*, and *At1g12520/CCS1*, a chaperone that activates CSD, as potential targets of miR398a (Table I). *CSD2* was not found, most likely due to a bulge and GU wobble in the seed region of the *CSD2* miR398a duplex (Brodersen and Voinnet, 2009).

## DISCUSSION

### qRT-PCR of pri-miRs Is Suitable for Discovery of Stimulus-Dependent miRs

The role of miRs during the adaptation of plants to abiotic and nutritional stresses is a field that attracts increasing interest (Chiou, 2007; Sunkar et al., 2007), but information on stress-dependent expression of *MIRNA* genes is limited. To overcome this situation, we developed a qRT-PCR platform for quantification of almost all known Arabidopsis pri-miRs. The results obtained with the platform and from targeted assays for mature miRs show that the responses of pri-miRs frequently match the responses of the biologically active mature species, thus validating pri-miR profiling as a useful discovery tool. It is also rapid, sensitive, and inexpensive and should represent an attractive initial approach for the investigation of *MIRNA* gene expression. The usefulness of the pri-miR platform is also demonstrated by comparative analysis of the *hyl1* mutant and wild-type plants, revealing accumulation of specific pri-miRs in *hyl1* and thus an important role

**Table I.** *Selected targets of P- and N-responsive miRs/miR*s*

| miR/miR* | Stimulus | Predicted Target Gene(s) | Gene Product(s) |
|---|---|---|---|
| 169a | +N (?) | Several *NF-YA*[abcdef] | Several nuclear factor Y A subunits |
| 169b/c | +N (?) | Several *NF-YA*[abcdef] | Several nuclear factor Y A subunits |
| | | At5g42120[abce] | Lectin protein kinase family protein |
| 169d to -g | +N (?) | Several *NF-YA*[abcdef] | Several nuclear factor Y A subunits |
| | | At1g70700[ae] and At1g48500[be] | Jasmonate-ZIM domain proteins 4 and 9 |
| 169h to -n | +N, +P | Several *NF-YA*[abcdef] | Several nuclear factor Y A subunits |
| | | At5g42120[ab] | Lectin protein kinase family protein |
| 398a | +P, +N, +C | At1g08830[bdef] | Cu/Zn superoxide dismutase CSD1 |
| | | At1g12520[be] | Superoxide dismutase chaperone CCS1 |
| | | At3g15640[cd] | Cytochrome *c* oxidase subunit COX5b.1 |
| 399a | −P | At2g33770[abcdef] | E2 conjugase PHO2 |
| | | At4g09730[ac] | ATP-dependent RNA helicase |
| | | At4g27850[e] | Pro-rich protein |
| 399b/c | −P | At2g33770[abcdef] | E2 conjugase PHO2 |
| | | At3g59420[abce] | ACR4 kinase |
| | | At3g54700[abc] | Phosphate transporter |
| | | At4g00170[bce] | VAMP family protein |
| | | At4g27850[e] | Pro-rich protein |
| | | At3g09922[e] | IPS1 |
| 399d | −P | At2g33770[abcdef] | E2 conjugase PHO2 |
| | | At4g09730[ac] | ATP-dependent RNA helicase |
| 399f | −P | At2g33770[abcdef] | E2 conjugase PHO2 |
| | | At3g09922[e] | IPS1 |
| 778 | −P | At2g22740[abcde] | Histone methyltransferase SUVH6 |
| | | At2g35160[a] | Histone methyltransferase SUVH5 |
| | | At5g51980[e] | WD40-repeat protein |
| 827 | −P | At1g02860[abcde] | SPX E3 ligase NLA |
| | | At1g63010[abce] | SPX E3 ligase |
| 2111 | −P | At3g27150[abce] | F box protein |
| | | At2g23370[abcde] | Unknown protein |
| | | At1g07010[abcde] | Calcineurin-like phosphoesterase |
| 398a* | +P, +N, +C | At4g00950[ae] | MEE47 (maternal effect embryo arrest 47) |
| | | At5g06120[abce] | Ran-binding protein |
| 399c* | −P | At5g64470[abe] | DUF231 protein |
| 399d* | −P | At3g11130[ae] | Clathrin heavy chain |
| 399f* | −P | At3g25905[abe] | CLAVATA3/ESR-RELATED27 |
| 778* | −P | Ag1g69610[abe] | Ribosomal protein |
| 2111a* | −P | At2g28290[e] | SWI2/SNF2-like protein SPLAYED |
| 2111b* | −P | At2g23380[abce] | SET domain protein CURLY LEAF |
| | | At1g60380[abe] | NAC domain transcription factor 24 |

[a]Predicted by miRU. [b]Predicted by WMD2. [c]Predicted by UEA toolbox. [d]Predicted by degradome data. [e]Predicted by PITA. [f]Experimentally confirmed.

for the HYL1 double-stranded RNA-binding protein in selective pri-miR maturation (Szarzynska et al., 2009). We found only a few examples where the P or N response of pri-miRs was not confirmed for the corresponding mature miRs. Although this could have been due to technical reasons, regulation or attenuation at the level of miR maturation could also account for these differences.

It is likely that the number of recognized Arabidopsis *MIRNA* loci will further increase (Lindow and Krogh, 2005; Lindow et al., 2007), especially with deeper analysis of SRS data, possibly reaching numbers similar to those currently known for rice (*Oryza sativa*; 269), zebra fish (337), mouse (472), and human (678; http://microrna.sanger.ac.uk). The easily scalable qRT-PCR approach allows regular updates of the platform as new *MIRNA* genes are discovered. In this regard, we invite readers to send us relevant sequence information.

### Evidence for miR2111 Being a True miR

The novel Pi-responsive miR2111 was revealed by a version of miRDeep optimized for analysis of plant sequences (P. May, unpublished data), but this alone is not conclusive proof that it is a true miR. A number of revised criteria exist for annotation of plant miRs (Meyers et al., 2008). The primary and only criterion that is necessary and sufficient for annotation as a miR is conclusive evidence of precise biogenesis from a qualifying stem loop, and this criterion is met by miR2111. First, miR2111 was shown to be derived from

longer poly(A)-tailed precursor transcripts, as it was possible to obtain precursor PCR amplicons from cDNA pools generated by RT with an oligo(dT) primer (Fig. 4C). Second, the two miR2111 precursors fold into characteristic hairpin structures with stabilities typical for known miR precursors. Third, there is precise excision of 21-nucleotide miR2111/miR2111* duplexes from the two stem-loop precursors (Supplemental File S3). Fourth, miR2111 and miR2111a/b* are derived from opposite stem arms and form duplexes with typical 3′ overhangs of two-nucleotide length. Fifth, base pairing between miR2111 and the star strands is extensive (Fig. 4B). Finally, the observed small RNA abundance corresponds entirely to the duplexes. Ancillary criteria for plant miR annotation include (1) the existence of target genes, (2) conservation between species, and (3) biogenesis that is dependent on DICER-like (DCL) proteins. There are obvious potential target genes for miR2111 (Table I), although the biological significance of these being targeted by miR2111 is as yet unknown. We also detected pre-miR2111 homologs and found mature miR2111 in rapeseed (Fig. 5; Supplemental Fig. S9). Although the dependence of miR2111 biogenesis on *DCL1* or *DCL4* still needs to be tested, there is already overwhelming evidence that miR2111 is a true miR.

### More Widespread Regulation by Small RNAs during P Limitation

So far, miR399s have been the only small RNA species known to strongly increase during P limitation (see introduction). Five *MIRNA399* genes that encode the slightly different mature miR399s exist in Arabidopsis. Still the only confirmed target of miR399s is *PHO2*, while *IPS1* is a miR399 interactor (Franco-Zorrilla et al., 2007). This situation and expansion of the *MIRNA399* gene family in other plant species such as *Medicago truncatula* (F. Krajinski, personal communication) and rice (Lindow et al., 2007), however, indicate a larger miR399 regulatory network. The new finding that at least four additional miRs and several miR*s with strong P status-dependent expression exist now suggests that regulation/signaling by small RNAs during P limitation is even more widespread. Regulatory activity of miR* species and their presence in argonaute complexes have been demonstrated previously (Mi et al., 2008; Okamura et al., 2008). The fact that the SRS read numbers for some miR* sequences clearly exceed the numbers for the corresponding miRs indicates that they are not merely by-products that are slowly degraded.

### Target Predictions and Biological Processes Potentially Affected by P-Regulated Small RNAs

We used several prediction algorithms and mined degradome data (Table I) to determine likely targets of P-regulated small RNAs. This combinatorial approach revealed several miR targets that were predicted by two or more complementary algorithms, giving greater confidence in the predictions. Target analysis with PITA also indicated that inclusion of thermodynamics of RNA-RNA interactions can change the results greatly (Hofacker, 2007). Only PITA correctly identified *IPS1*, a noncoding RNA that qualifies as a bona fide miR399 target-like interactor (Franco-Zorrilla et al., 2007), emphasizing the complementarity and predictive power of PITA. The number of potential targets identified with PITA (Supplemental File S4) further suggests that an individual plant miR could also have a larger range of action, for example, by inducing widespread changes in protein synthesis, as recently reported for several human miRs (Selbach et al., 2008).

Three P starvation-inducible miRs (miR399, miR2111, and miR827) have confirmed or likely target genes involved in protein degradation via the 26S proteasome. MiR827 targets the E3 ligase gene *NLA* (*At1g02860*). *NLA* transcript also drops 2- to 3-fold during P limitation when miR827 is highly expressed (Morcuende et al., 2007). NLA is crucial for anthocyanin synthesis, and the *nla* mutant displays severely reduced anthocyanin content and early leaf senescence during N limitation (Peng et al., 2007a, 2007b, 2008). However, during P limitation or during simultaneous P and N limitation, the mutant displays wild-type-like anthocyanin levels and no leaf senescence (Peng et al., 2008), showing that the signal derived from P limitation is sufficient to induce anthocyanin production in

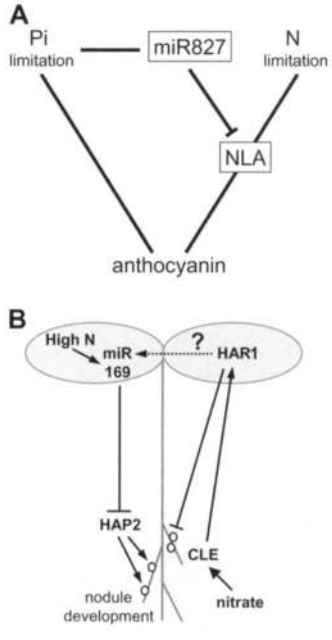


**Figure 6.** Hypothetical models for miR827 and miR169 functions. A, Model showing cross talk between P limitation and N limitation signaling pathways that affect anthocyanin synthesis. B, Model integrating published features of the systemic regulation of nodulation by CLE (Okamoto et al., 2009), SUNN/HAR1 (Krusell et al., 2002), and HAP2 and miR169 (Combier et al., 2006), with novel results concerning miR169 described in this work.

the *nla* mutant. The link between P limitation and *NLA* provided by miR827 (Fig. 6A) suggests that NLA activity is actively down-regulated during P limitation. This could indicate that plants select one or the other input signal depending on nutrient conditions and, therefore, the existence of hierarchies in the interplay of macronutrient regulatory networks. MiR2111 is predicted to target the E3 ligase gene *At3g27150* (Table I). *At3g27150* displays strictly root-specific expression in large-scale transcriptome data sets like AtGenExpress (Schmid et al., 2005), suggesting that it functions in the root. This is interesting in the context of the high abundance of miR2111 in phloem sap during Pi limitation (Fig. 5), suggesting another systemic regulatory circuitry, analogous to the miR399-*PHO2* paradigm (Pant et al., 2008).

Regulation of chromatin status appears to be another biological process influenced by P limitation-induced miRs, as suggested by the best predicted target genes of miR778, miR2111b*, and miR2111a*, namely *SUVH6* (*At2g22740*), encoding a SET domain-containing histone methyltransferase; *At2g23380/CURLY LEAF*, a SET domain gene required for histone methylation and genetic imprinting (Schubert et al., 2006); and *At2g28290/SPLAYED*, encoding a chromatin-remodeling complex subunit required for maintenance and identity of the shoot apical meristem (Kwon et al., 2005).

MiR398a is strongly reduced in P, N, and C limitation (Fig. 3), indicating a more general response to nutrient stress. Repression of miR398a by C limitation also correlates with its induction by Suc (Dugas and Bartel, 2008). Targets of miR398a include *CSD1* and *CSD2* (see introduction). CSD is required for detoxification of reactive oxygen species that increase during nutrient limitations and other environmental stresses (e.g. heat or drought; Apel and Hirt, 2004; Shin et al., 2005; Sunkar et al., 2006). Therefore, down-regulation of miR398a leading to higher CSD activity would be an appropriate response to nutrient stress.

### Potential Biological Impact of miR169 Regulation by N Availability

The targets of miR169s are several HAP2 transcription factors (i.e. nuclear factor YA subunits [NF-YA]; Table I; Combier et al., 2006; Fahlgren et al., 2007; Li et al., 2008). Transcripts of several of these genes, including *At3g05690/NF-YA2*, *At1g54160/NF-YA5*, *At3g14020/NF-YA6*, *At1g72830/NF-YA8*, and *At5g06510/NF-YA10*, increase during N and P limitation (Supplemental Fig. S10; Scheible et al., 2004; qRT-PCR confirmation not shown), thereby showing the opposite response compared with miR169.

In Arabidopsis, miR169 was reported to influence drought resistance via inhibition of the A5 subunit of NF-Y, a ubiquitous transcription factor that is highly expressed in guard cells and crucial for the expression of a number of drought stress-responsive genes (Li et al., 2008). *Nfya5* knockout mutants and plants over-expressing miR169 show enhanced leaf water loss and are more sensitive to drought stress, whereas *NFYA5* overexpressers show the opposite phenotypes (Li et al., 2008). In addition to the effects of the nitrate transporter CHL1 (Guo et al., 2003) or nitrate reductase-mediated nitric oxide generation (Desikan et al., 2002) on stomatal opening, low expression of miR169 during N limitation could thus contribute to drought tolerance of N-limited plants (Lodeiro et al., 2000; Castaings et al., 2008).

In legume species, nodule development is dependent on the presence of previously established nodules and N/nitrate availability, creating a root-to-shoot signal that activates the CLAVATA1-like receptor kinase SUNN in *M. truncatula* or HAR1 in *Lotus japonicus*. A recent report suggests that a nitrate-induced CLAVATA3/ESR-related (CLE) peptide is this root-to-shoot signal (Fig. 6B; Okamoto et al., 2009). HAR1 exerts negative shoot control of root nodulation (Krusell et al., 2002; Nishimura et al., 2002) through a shoot-to-root signal that might include auxin transport (van Noorden et al., 2006). It is also known that the miR169 target gene *HAP2-1* in *M. truncatula* is a key regulator for the differentiation of nodule primordia (Combier et al., 2006; Fig. 6B). MiR169 overexpression or knockdown of *HAP2-1* leads to a developmental block of nodule formation (Combier et al., 2006). Repression of miR169s by N limitation, as detected in our experiments, points toward a potential mechanistic link between low N status and nodule development in legumes. High abundance of miR169 in phloem sap during N-replete growth and the sharp decrease during N and P limitation (Fig. 5) also flags miR169 as a potential long-distance signal (Fig. 6B) that is able to report shoot N and P status to the roots, similar to the role of miR399 (Pant et al., 2008). It will be interesting to test whether miR169 abundance is increased by nitrate/N in legumes and whether miR169 expression and/or phloem abundance is dependent on *SUNN/HAR1* to establish if this is a novel shoot-to-root signal for the control of nodule differentiation.

## CONCLUSION

MiRs are emerging as increasingly interesting (systemic) regulators during mineral nutrient stress in plants. The discovery of new nutrient-dependent miRs opens up the possibility of testing their roles and those of their predicted targets during adaptation of plants to nutrient deficiency. The qRT-PCR platform described here serves as a useful initial approach to test the response of annotated miRs in a given biological scenario, providing opportunities to discover new signaling and regulatory networks.

## MATERIALS AND METHODS

### Plant Materials

Nine-day-old nutrient-replete and N-, P-, or C-limited wild-type Arabidopsis (*Arabidopsis thaliana* Col-0) seedlings were grown in sterile liquid

cultures as described previously (Scheible et al., 2004; Morcuende et al., 2007; Osuna et al., 2007). The physiological status of the plant materials was confirmed by expression analysis of marker genes (Supplemental Fig. S5) prior to qRT-PCR analysis. Rapeseed (*Brassica napus* 'Drakkar') was germinated and grown hydroponically (Buhtz et al., 2008) in a full-nutrient solution containing 4 mM N and 0.5 mM P. After 47 d, plants were divided into three sets, and one set was supplied with lower N (2 mM $KNO_3$) nutrient solution, one with low P (0.1 M KPi) nutrient solution, and one with full-nutrient solution. From day 61 onward (i.e. approximately 1 week before flowering started), low-N, low-P, and FN plants were supplied with nutrient solutions containing no N, no P, or full-nutrient solution, respectively. N- or P-limited plants developed clear signs of N or P starvation (e.g. reduced leaf biomass, earlier flowering, reduced chlorophyll in −N leaves; data not shown). Phloem sap was sampled between days 72 and 82 as described previously and was not significantly contaminated by cell sap from other tissues (Giavalisco et al., 2006; Buhtz et al., 2008).

## Primer Design and qRT-PCR Analysis

A first set of pri-miR primers (pri-miR156 through -404) was designed by Eurogentec. Primers for pri-miR405 through -870, and primers that replaced malfunctioning primers from the first set were designed using Primer Express 2.0.0 (Applied Biosystems) and Oligo 6.71 (Molecular Biology Insights). To ensure maximum specificity and efficiency during PCR amplification of pri-miR cDNA under a standard set of reaction conditions (Fig. 1A), a stringent set of criteria was used for primer design. This included predicted melting temperatures of 61°C ± 2°C, limited self-complementarity, and PCR amplicon lengths of 50 to 150 bp. Secondary hits were minimized by aligning primer candidates to all known Arabidopsis transcript sequences via BLAST searches and eliminating primer pairs with more than the specific hit. Stem-loop sequences for which no satisfactory primers could be found were elongated by 100 bp of flanking genomic sequence on each side before primer design was reinitiated. Annealing sites of the primers on the pri-miR sequence are highlighted in Supplemental File S1. Sequences of the qRT-PCR primers are given in Supplemental File S2. Cartridge-purified primers were purchased from Eurogentec, mixed with the corresponding forward or reverse primer upon arrival to a final concentration of 50 μM each, arrayed on 96-deep-well plates, and frozen at −80°C for long-term storage. Working stocks (0.5 μM) of each primer pair were prepared from the storage stocks in two serial 10-fold dilution steps and kept at −20°C for short-term storage and used within 2 weeks.

RNA isolation, cDNA synthesis, and qRT-PCR analysis were carried out as described previously by Czechowski et al. (2004, 2005) and Udvardi et al. (2008). Mature miR expression was analyzed using the method of Chen et al. (2005), as described (Pant et al., 2008). MiR-specific RT stem-loop primers are given in Supplemental Table S1. Primer sequences for marker genes are given in the legend to Supplemental Figure S5.

## Isolation of Small RNAs, Library Preparation, and Deep Sequencing

Total RNA was isolated with Trizol reagent (Invitrogen) supplemented with 0.5% (w/v) *N*-lauroylsarcosine sodium salt, 3 mM β-mercaptoethanol, and 5 mM EDTA. After phase separation, one phenol/chloroform and two chloroform extractions were performed. The aqueous phase (500 μL) was mixed with 3 μL of glycogen (Roche; 20 mg $mL^{-1}$) before RNA was precipitated with 625 μL of ethanol and 250 μL of 0.8 M sodium citrate/1.2 M sodium chloride. Samples were incubated for 30 min at room temperature and then centrifuged (25 min, 16,000*g*, 4°C). The precipitate was washed with 80% (v/v) ethanol, air dried, and dissolved in 2 mM Tris-HCl (pH 7.5). Efficiency of small RNA extraction and total RNA quality was checked by northern-blot hybridization with a $^{32}$P-labeled oligonucleotide complementary to miR399 (Bari et al., 2006). RNA concentration was measured with a NanoDrop ND-1000 (NanoDrop Technologies), and integrity was measured with an Agilent-2100 Bioanalyzer (Agilent Technologies; RNA 6000 NanoChips).

Total RNA from three independent biological replicates (3 × 20 μg) was mixed with 2× loading buffer II (Ambion), denatured for 2 min at 90°C, and separated on a 15% polyacrylamide/7 M urea/1× TBE gel at 300 V. Synthetic, phosphorylated 18-mer and 24-mer RNA markers (Biomers.net) and a 10-bp DNA ladder (Invitrogen) were used to localize small RNAs (18–30 nucleotides) as well as ligation and PCR products on gels stained with SYBR Gold (Invitrogen). RNA and PCR products were eluted from polyacrylamide gels in 300 μL of EBR buffer (50 mM Mg acetate, 0.5 M ammonium acetate, 1 mM EDTA, and 0.1% SDS) for 10 to 16 h at 20°C to 25°C (300 rpm). After phenol/chloroform and chloroform extraction, the aqueous phase was mixed with 1 μL of glycogen and 900 μL of 96% (v/v) ethanol, then cooled to −20°C for 2 h and centrifuged (25 min, 16,000*g*, 4°C). The RNA pellet was washed twice with 75% (v/v) ethanol and dissolved in 6 μL of water.

5′ and 3′ RNA adaptor ligations with RNA primers, RT, and PCR were performed according to Lu et al. (2007), except for a 3′ RNA adaptor 3′ end modification consisting of a C3 hydrocarbon spacer (Biomers.net). The PCR (25 μL) was terminated with 75 μL of stop buffer (10 mM Tris-HCl, pH 8.0, 1 mM EDTA, and 0.4 M ammonium acetate). After phenol (pH = 8.0)/chloroform extraction, 1 μL of glycogen (Roche; 20 mg $mL^{-1}$) and 300 μL of ethanol were added to precipitate cDNA. The cDNA was denatured in loading buffer II (Ambion) and separated on an 8% polyacrylamide/7 M urea gel. The cDNA band was eluted and precipitated as above. The pellet was washed with 70% (v/v) ethanol, air dried, and dissolved in 14 μL of water. The cDNA concentration was measured using a NanoDrop ND-1000 and checked by 15% polyacrylamide/7 M urea gel electrophoresis with oligonucleotides of known concentration. Quality control was performed by TOPO cloning and Sanger sequencing of several plasmid clones (Lu et al., 2007). Illumina-Solexa sequencing was performed at GATC Biotech for Arabidopsis and at FASTERIS for rapeseed libraries.

## Analysis of Deep Sequencing Results

Sequencing reads of lengths between 15 and 32 nucleotides were used after trimming sequence adapters and low-complexity regions [e.g. poly(A)] and after removing reads of low quality (containing *n* runs, where $n > 12$). The read sets from the different conditions were subsequently mapped onto the Arabidopsis genome (TAIR8 assembly) using RazerS software. RazerS is an efficient and generic read-mapping tool allowing the user to align reads of arbitrary length using either the Hamming distance or the edit distance. RazerS is part of the generic sequence analysis library Seqan (Doring et al., 2008). Only perfect matches to the genome (i.e. full-length alignments with 100% identity) were retained. To investigate the read distributions for available TAIR8 annotations of genes and transposable elements (available from ftp://ftp.arabidopsis.org/home/tair/Genes/TAIR8_genome_release) and to find statistically significant changes in read distributions, we used the $\chi^2$ test together with Benjamini-Hochberg *P* value correction. The $\chi^2$ test is known to have a good predictive power and robustness for gene expression analysis (Man et al., 2000). Normalization of small RNA data was performed by dividing the read number of each individual small RNA sequence by the number of redundant reads (15–32 nucleotides) in each library (Supplemental Tables S2 and S3).

## MiR Prediction

Potential miRs together with their precursor sequences were predicted using the miRDeep software tool (Friedländer et al., 2008). The miRDeep algorithm was adjusted to plant precursor structures to take account of the following features of some plant miRs: (1) longer pre-miRs; (2) pre-miRs that contain more than one miR sequence; (3) the more diverse read distribution of sequenced small RNAs on plant pre-miR sequences; and (4) nonhairpin pre-miR structures (P. May, unpublished data).

## Target Gene Predictions

Candidate miR target genes were determined using publicly available prediction algorithms, including miRU (Zhang, 2005), the target search in WMD2 (Ossowski et al., 2008), the prediction tool in the UEA plant sRNA toolkit (Moxon et al., 2008b), and PITA (Kertesz et al., 2007). The programs were used with their default settings.

MiRBase accession numbers for all annotated Arabidopsis miRs are available at http://microrna.sanger.ac.uk/cgi-bin/sequences/mirna_summary.pl?org=ath. GenBank accession numbers for the novel miR2111 sequences described in this work are FN391952 (Ath-miR2111b), FN391950 (Ath-miR2111a), FN391951 (Bna-miR2111b), and FN391953 (Bna-miR2111a).

## Supplemental Data

The following materials are available in the online version of this article.

**Supplemental Figure S1.** Genome arrangement and sequence similarity of miR169i to -n precursors.

**Supplemental Figure S2.** Strong induction of mir395 primary transcripts during sulfur limitation.

**Supplemental Figure S3.** Melting curves of pri-miR amplicons

**Supplemental Figure S4.** Sequencing results of four pri-miR amplicons.

**Supplemental Figure S5.** Marker gene expression in nutrient-limited Arabidopsis seedlings.

**Supplemental Figure S6.** Strong overexpression of miR399d mimics molecular phenotypes of *pho2* mutants.

**Supplemental Figure S7.** Number and length distribution of small RNA sequences.

**Supplemental Figure S8.** qRT-PCR verification of P limitation-induced small RNA species.

**Supplemental Figure S9.** miR2111 precursors from rapeseed.

**Supplemental Figure S10.** Nutrient-dependent expression of HAP2 genes in Arabidopsis.

**Supplemental Table S1.** Primers used for RT of mature miR and qPCR quantification.

**Supplemental Table S2.** Read numbers from small RNA sequencing of Arabidopsis libraries.

**Supplemental Table S3.** Read numbers from small RNA sequencing of rapeseed phloem sap.

**Supplemental File S1.** Arabidopsis miR precursor sequences and primer annealing sites.

**Supplemental File S2.** Quantitative real-time PCR results for all investigated pri-miR species.

**Supplemental File S3.** Structures and small RNA reads of P-responsive miRs.

**Supplemental File S4.** Target gene predictions.

## Note Added in Proof

The novel miR described in this work was independently reported by Fahlgren et al. (**Fahlgren N, Sullivan CM, Kasschau KD, Chapman EJ, Cumbie JS, Montgomery TA, Gilbert SD, Dasenko M, Backman TW, Givan SA, et al** [2009] Computational and analytical framework for small RNA profiling by high-throughput sequencing. RNA **15:** 992–1002). To unify the naming, this miR is referred to as miR2111 in the final published version.

## ACKNOWLEDGMENTS

We thank Dr. John Lunn (Max-Planck Institute of Molecular Plant Physiology) and Dr. Peter Dörner (University of Edinburgh) for proofreading and suggestions on the manuscript.

Received March 27, 2009; accepted May 18, 2009; published May 22, 2009.

## LITERATURE CITED

**Addo-Quaye C, Eshoo TW, Bartel DP, Axtell MJ** (2008) Endogenous siRNA and miRNA targets identified by sequencing of the Arabidopsis degradome. Curr Biol **18:** 758–762

**Allen E, Xie Z, Gustafson AM, Carrington JC** (2005) MicroRNA-directed phasing during trans-acting siRNA biogenesis in plants. Cell **121:** 207–221

**Apel K, Hirt H** (2004) Reactive oxygen species: metabolism, oxidative stress, and signal transduction. Annu Rev Plant Biol **55:** 373–399

**Aukerman MJ, Sakai H** (2003) Regulation of flowering time and floral organ identity by a microRNA and its APETALA2-like target genes. Plant Cell **15:** 2730–2741

**Aung K, Lin SI, Wu CC, Huang YT, Su CL, Chiou TJ** (2006) Pho2, a phosphate overaccumulator, is caused by a nonsense mutation in a microRNA399 target gene. Plant Physiol **141:** 1000–1011

**Axtell MJ, Bartel DP** (2005) Antiquity of microRNAs and their targets in land plants. Plant Cell **17:** 1658–1673

**Bari R, Pant BD, Stitt M, Scheible WR** (2006) PHO2, microRNA399, and PHR1 define a phosphate-signaling pathway in plants. Plant Physiol **141:** 988–999

**Bartel DP** (2004) MicroRNAs: genomics, biogenesis, mechanism, and function. Cell **116:** 281–297

**Bracht J, Hunter S, Eachus R, Weeks P, Pasquinelli AE** (2004) Trans-splicing and polyadenylation of let-7 microRNA primary transcripts. RNA **10:** 1586–1594

**Brodersen P, Sakvarelidze-Achard L, Bruun-Rasmussen M, Dunoyer P, Yamamoto YY, Sieburth L, Voinnet O** (2008) Widespread translational inhibition by plant miRNAs and siRNAs. Science **320:** 1185–1190

**Brodersen P, Voinnet O** (2009) Revisiting the principles of microRNA target recognition and mode of action. Nat Rev Mol Cell Biol **10:** 141–148

**Buhtz A, Springer F, Chappell L, Baulcombe DC, Kehr J** (2008) Identification and characterization of small RNAs from the phloem of Brassica napus. Plant J **53:** 739–749

**Cai X, Hagedorn CH, Cullen BR** (2004) Human microRNAs are processed from capped, polyadenylated transcripts that can also function as mRNAs. RNA **10:** 1957–1966

**Castaings L, Camargo A, Pocholle D, Gaudon V, Texier Y, Boutet-Mercey S, Taconnat L, Renou JP, Daniel-Vedele F, Fernandez E, et al** (2008) The nodule inception-like protein 7 modulates nitrate sensing and metabolism in Arabidopsis. Plant J **57:** 426–435

**Chen C, Ridzon DA, Broomer AJ, Zhou Z, Lee DH, Nguyen JT, Barbisin M, Xu NL, Mahuvakar VR, Andersen MR, et al** (2005) Real-time quantification of microRNAs by stem-loop RT-PCR. Nucleic Acids Res **33:** e179

**Chiou TJ** (2007) The role of microRNAs in sensing nutrient stress. Plant Cell Environ **30:** 323–332

**Chiou TJ, Aung K, Lin SI, Wu CC, Chiang SF, Su CL** (2006) Regulation of phosphate homeostasis by microRNA in *Arabidopsis*. Plant Cell **18:** 412–421

**Chuck G, Candela H, Hake S** (2009) Big impacts by small RNAs in plant development. Curr Opin Plant Biol **12:** 81–86

**Combier JP, Frugier F, de Billy F, Boualem A, El-Yahyaoui F, Moreau S, Vernié T, Ott T, Gamas P, Crespi M, et al** (2006) MtHAP2-1 is a key transcriptional regulator of symbiotic nodule development regulated by microRNA169 in Medicago truncatula. Genes Dev **20:** 3084–3088

**Czechowski T, Bari RP, Stitt M, Scheible WR, Udvardi MK** (2004) Real-time RT-PCR profiling of over 1400 Arabidopsis transcription factors: unprecedented sensitivity reveals novel root- and shoot-specific genes. Plant J **38:** 366–379

**Czechowski T, Stitt M, Altmann T, Udvardi MK, Scheible WR** (2005) Genome-wide identification and testing of superior reference genes for transcript normalization in Arabidopsis. Plant Physiol **139:** 5–17

**Desikan R, Griffiths R, Hancock J, Neill S** (2002) A new role for an old enzyme: nitrate reductase-mediated nitric oxide generation is required for abscisic acid-induced stomatal closure in Arabidopsis thaliana. Proc Natl Acad Sci USA **99:** 16314–16318

**De Smet I, Vassileva V, De Rybel B, Levesque MP, Grunewald W, Van Damme D, van Noorden G, Naudts M, Van Isterdael G, De Clercq R, et al** (2008) Receptor-like kinase ACR4 restricts formative cell divisions in the Arabidopsis root. Science **322:** 594–597

**Doring A, Weese D, Rausch T, Reinert K** (2008) SeqAn an efficient, generic C++ library for sequence analysis. BMC Bioinformatics **9:** 11

**Dugas DV, Bartel B** (2004) MicroRNA regulation of gene expression in plants. Curr Opin Plant Biol **7:** 512–520

**Dugas DV, Bartel B** (2008) Sucrose induction of Arabidopsis miR398 represses two Cu/Zn superoxide dismutases. Plant Mol Biol **67:** 403–417

**Emery JF, Floyd SK, Alvarez J, Eshed Y, Hawker NP, Izhaki A, Baum SF, Bowman JL** (2003) Radial patterning of Arabidopsis shoots by class III HD-ZIP and KANADI genes. Curr Biol **13:** 1768–1774

**Fahlgren N, Howell MD, Kasschau KD, Chapman EJ, Sullivan CM, Cumbie JS, Givan SA, Law TF, Grant SR, Dangl JL, et al** (2007) High-throughput sequencing of Arabidopsis microRNAs: evidence for frequent birth and death of MIRNA genes. PLoS ONE **2:** e219

**Franco-Zorrilla JM, Valli A, Todesco M, Mateos I, Puga MI, Rubio-Somoza I, Leyva A, Weigel D, García JA, Paz-Ares J** (2007) Target mimicry provides a new mechanism for regulation of microRNA activity. Nat Genet **39:** 1033–1037

**Friedländer MR, Chen W, Adamidi C, Maaskola J, Einspanier R, Knespel S, Rajewsky N** (2008) Discovering microRNAs from deep sequencing data using miRDeep. Nat Biotechnol **26:** 407–415

**Fujii H, Chiou TJ, Lin SI, Aung K, Zhu JK** (2005) A miRNA involved in phosphate-starvation response in Arabidopsis. Curr Biol **15:** 2038–2042

**German MA, Pillay M, Jeong DH, Hetawal A, Luo S, Janardhanan P, Kannan V, Rymarquis LA, Nobuta K, German R, et al** (2008) Global identification of microRNA-target RNA pairs by parallel analysis of RNA ends. Nat Biotechnol **26:** 941–946

**Giavalisco P, Kapitza K, Kolasa A, Buhtz A, Kehr J** (2006) Towards the proteome of Brassica napus phloem sap. Proteomics **6:** 896–909

**Gifford ML, Dean A, Gutierrez RA, Coruzzi GM, Birnbaum KD** (2008) Cell-specific nitrogen responses mediate developmental plasticity. Proc Natl Acad Sci USA **105:** 803–808

**Guo FQ, Young J, Crawford NM** (2003) The nitrate transporter AtNRT1.1 (CHL1) functions in stomatal opening and contributes to drought susceptibility in *Arabidopsis*. Plant Cell **15:** 107–117

**Hofacker IL** (2007) How microRNAs choose their targets. Nat Genet **39:** 1191–1192

**Jones-Rhoades MW, Bartel DP** (2004) Computational identification of plant microRNAs and their targets, including a stress-induced miRNA. Mol Cell **14:** 787–799

**Kawashima CG, Yoshimoto N, Maruyama-Nakashita A, Tsuchiya YN, Saito K, Takahashi H, Dalmay T** (2008) Sulphur starvation induces the expression of microRNA-395 and one of its target genes but in different cell types. Plant J **57:** 313–321

**Kertesz M, Iovino N, Unnerstall U, Gaul U, Segal E** (2007) The role of site accessibility in microRNA target recognition. Nat Genet **39:** 1278–1284

**Kidner CA, Martienssen RA** (2005) The developmental role of microRNA in plants. Curr Opin Plant Biol **8:** 38–44

**Krusell L, Madsen LH, Sato S, Aubert G, Genua A, Szczyglowski K, Duc G, Kaneko T, Tabata S, de Bruijn F, et al** (2002) Shoot control of root development and nodulation is mediated by a receptor-like kinase. Nature **420:** 422–426

**Kurihara Y, Watanabe Y** (2004) Arabidopsis micro-RNA biogenesis through Dicer-like 1 protein functions. Proc Natl Acad Sci USA **101:** 12753–12758

**Kutter C, Schöb H, Stadler M, Meins F Jr, Si-Ammour A** (2007) MicroRNA-mediated regulation of stomatal development in *Arabidopsis*. Plant Cell **19:** 2417–2429

**Kwon CS, Chen C, Wagner D** (2005) WUSCHEL is a primary target for transcriptional regulation by SPLAYED in dynamic control of stem cell fate in Arabidopsis. Genes Dev **19:** 992–1003

**Lai EC** (2004) Predicting and validating microRNA targets. Genome Biol **5:** 115

**Lee Y, Kim M, Han J, Yeom KH, Lee S, Baek SH, Kim VN** (2004) MicroRNA genes are transcribed by RNA polymerase II. EMBO J **23:** 4051–4060

**Li WX, Oono Y, Zhu J, He XJ, Wu JM, Iida K, Lu XY, Cui X, Jin H, Zhu JK** (2008) The *Arabidopsis* NFYA5 transcription factor is regulated transcriptionally and posttranscriptionally to promote drought resistance. Plant Cell **20:** 2238–2251

**Lin SI, Chiang SF, Lin WY, Chen JW, Tseng CY, Wu PC, Chiou TJ** (2008) Regulatory network of microRNA399 and PHO2 by systemic signaling. Plant Physiol **147:** 732–746

**Lindow M, Jacobsen A, Nygaard S, Mang Y, Krogh A** (2007) Intragenomic matching reveals a huge potential for miRNA-mediated regulation in plants. PLoS Comput Biol **3:** e238

**Lindow M, Krogh A** (2005) Computational evidence for hundreds of non-conserved plant microRNAs. BMC Genomics **13:** 119

**Liu HH, Tian X, Li YJ, Wu CA, Zheng CC** (2008) Microarray-based analysis of stress-regulated microRNAs in Arabidopsis thaliana. RNA **14:** 836–843

**Lodeiro AR, González P, Hernández A, Balagué LJ, Favelukes G** (2000) Comparison of drought tolerance in nitrogen-fixing and inorganic nitrogen-grown common beans. Plant Sci **154:** 31–41

**Lu C, Meyers BC, Green PJ** (2007) Construction of small RNA cDNA libraries for deep sequencing. Methods **43:** 110–117

**Man MZ, Wang X, Wang Y** (2000) POWER_SAGE: comparing statistical tests for SAGE experiments. Bioinformatics **16:** 953–959

**Meyers BC, Axtell MJ, Bartel B, Bartel DP, Baulcombe D, Bowman JL, Cao X, Carrington JC, Chen X, Green PJ, et al** (2008) Criteria for annotation of plant microRNAs. Plant Cell **20:** 3186–3190

**Mi S, Cai T, Hu Y, Chen Y, Hodges E, Ni F, Wu L, Li S, Zhou H, Long C, et al** (2008) Sorting of small RNAs into Arabidopsis argonaute complexes is directed by the 5′ terminal nucleotide. Cell **133:** 116–127

**Morcuende R, Bari R, Gibon Y, Zheng W, Pant BD, Bläsing O, Usadel B, Czechowski T, Udvardi MK, Stitt M, et al** (2007) Genome-wide reprogramming of metabolism and regulatory networks of Arabidopsis in response to phosphorus. Plant Cell Environ **30:** 85–112

**Moxon S, Jing R, Szittya G, Schwach F, Rusholme P, Pilcher RL, Moulton V, Dalmay T** (2008a) Deep sequencing of tomato short RNAs identifies microRNAs targeting genes involved in fruit ripening. Genome Res **18:** 1602–1609

**Moxon S, Schwach F, Dalmay T, Maclean D, Studholme DJ, Moulton V** (2008b) A toolkit for analysing large-scale plant small RNA datasets. Bioinformatics **24:** 2252–2253

**Nishimura R, Hayashi M, Wu GJ, Kouchi H, Imaizumi-Anraku H, Murakami Y, Kawasaki S, Akao S, Ohmori M, Nagasawa M, et al** (2002) HAR1 mediates systemic regulation of symbiotic organ development. Nature **420:** 426–429

**Okamoto S, Ohnishi E, Sato S, Takahashi H, Nakazono M, Tabata S, Kawaguchi M** (2009) Nod factor/nitrate-induced CLE genes that drive HAR1-mediated systemic regulation of nodulation. Plant Cell Physiol **50:** 67–77

**Okamura K, Phillips MD, Tyler DM, Duan H, Chou YT, Lai EC** (2008) The regulatory activity of microRNA* species has substantial influence on microRNA and 3′ UTR evolution. Nat Struct Mol Biol **15:** 354–363

**Ossowski S, Schwab R, Weigel D** (2008) Gene silencing in plants using artificial microRNAs and other small RNAs. Plant J **53:** 674–690

**Osuna D, Usadel B, Morcuende R, Gibon Y, Bläsing OE, Höhne M, Günter M, Kamlage B, Trethewey R, Scheible WR, et al** (2007) Temporal responses of transcripts, enzyme activities and metabolites after adding sucrose to carbon-deprived Arabidopsis seedlings. Plant J **49:** 463–491

**Palatnik JF, Allen E, Wu X, Schommer C, Schwab R, Carrington JC, Weigel D** (2003) Control of leaf morphogenesis by microRNAs. Nature **425:** 257–263

**Pant BD, Buhtz A, Kehr J, Scheible WR** (2008) MicroRNA399 is a long-distance signal for the regulation of plant phosphate homeostasis. Plant J **53:** 731–738

**Peng M, Bi YM, Zhu T, Rothstein SJ** (2007a) Genome-wide analysis of Arabidopsis responsive transcriptome to nitrogen limitation and its regulation by the ubiquitin ligase gene NLA. Plant Mol Biol **65:** 775–797

**Peng M, Hannam C, Gu H, Bi YM, Rothstein SJ** (2007b) A mutation in NLA, which encodes a RING-type ubiquitin ligase, disrupts the adaptability of Arabidopsis to nitrogen limitation. Plant J **50:** 320–337

**Peng M, Hudson D, Schofield A, Tsao R, Yang R, Gu H, Bi YM, Rothstein SJ** (2008) Adaptation of Arabidopsis to nitrogen limitation involves induction of anthocyanin synthesis which is controlled by the NLA gene. J Exp Bot **59:** 2933–2944

**Ramakers C, Ruijter JM, Deprez RH, Moorman AF** (2003) Assumption-free analysis of quantitative real-time polymerase chain reaction (PCR) data. Neurosci Lett **339:** 62–66

**Rhoades MW, Reinhart BJ, Lim LP, Burge CB, Bartel B, Bartel DP** (2002) Prediction of plant microRNA targets. Cell **110:** 513–520

**Scheible WR, Morcuende R, Czechowski T, Fritz C, Osuna D, Palacios-Rojas N, Schindelasch D, Thimm O, Udvardi MK, Stitt M** (2004) Genome-wide reprogramming of primary and secondary metabolism, protein synthesis, cellular growth processes, and the regulatory infrastructure of Arabidopsis in response to nitrogen. Plant Physiol **136:** 2483–2499

**Schmid M, Davison TS, Henz SR, Pape UJ, Demar M, Vingron M, Schölkopf B, Weigel D, Lohmann JU** (2005) A gene expression map of Arabidopsis thaliana development. Nat Genet **37:** 501–506

**Schmittgen TD, Jiang J, Liu Q, Yang L** (2004) A high-throughput method to monitor the expression of microRNA precursors. Nucleic Acids Res **32:** e43

**Schubert D, Primavesi L, Bishopp A, Roberts G, Doonan J, Jenuwein T,**

**Goodrich J** (2006) Silencing by plant Polycomb-group genes requires dispersed trimethylation of histone H3 at lysine 27. EMBO J **25:** 4638–4649

**Selbach M, Schwanhäuser B, Thierfelder N, Fang Z, Khanin R, Rajewsky N** (2008) Widespread changes in protein synthesis by microRNAs. Nature **455:** 58–63

**Sharma VK, Ramirez J, Fletcher JC** (2003) The Arabidopsis CLV3-like (CLE) genes are expressed in diverse tissues and encode secreted proteins. Plant Mol Biol **51:** 415–425

**Shi R, Chiang VL** (2005) Facile means for quantifying microRNA expression by real-time PCR. Biotechniques **39:** 519–525

**Shin R, Berg RH, Schachtman DP** (2005) Reactive oxygen species and root hairs in Arabidopsis root response to nitrogen, phosphorus and potassium deficiency. Plant Cell Physiol **46:** 1350–1357

**Sunkar R, Chinnusamy V, Zhu J, Zhu JK** (2007) Small RNAs as big players in plant abiotic stress responses and nutrient deprivation. Trends Plant Sci **12:** 301–309

**Sunkar R, Kapoor A, Zhu JK** (2006) Posttranscriptional induction of two Cu/Zn superoxide dismutase genes in *Arabidopsis* is mediated by downregulation of miR398 and important for oxidative stress tolerance. Plant Cell **18:** 2051–2065

**Sunkar R, Zhu JK** (2004) Novel and stress-regulated microRNAs and other small RNAs from *Arabidopsis*. Plant Cell **16:** 2001–2019

**Szarzynska B, Sobkowiak L, Pant BD, Balazadeh S, Scheible W-R, Mueller-Roeber B, Jarmolowski A, Szweykowska-Kulinska Z** (2009) Gene structures and processing of Arabidopsis thaliana HYL1-dependent pri-miRNAs. Nucleic Acids Res **9:** 3083–3093

**Szittya G, Moxon S, Santos DM, Jing R, Fevereiro MP, Moulton V, Dalmay T** (2008) High-throughput sequencing of Medicago truncatula short RNAs identifies eight new miRNA families. BMC Genomics **9:** 593

**Udvardi MK, Czechowski T, Scheible WR** (2008) Eleven golden rules of quantitative RT-PCR. Plant Cell **20:** 1736–1737

**van Noorden GE, Ross JJ, Reid JB, Rolfe BG, Mathesius U** (2006) Defective long-distance auxin transport regulation in the *Medicago truncatula* super numeric nodules mutant. Plant Physiol **140:** 1494–1506

**Wu G, Poethig RS** (2006) Temporal regulation of shoot development in Arabidopsis thaliana by miR156 and its target SPL3. Development **133:** 3539–3547

**Yamasaki H, Abdel-Ghany SE, Cohu CM, Kobayashi Y, Shikanai T, Pilon M** (2007) Regulation of copper homeostasis by micro-RNA in Arabidopsis. J Biol Chem **282:** 16369–16378

**Yoo BC, Kragler F, Varkonyi-Gasic E, Haywood V, Archer-Evans S, Lee YM, Lough TJ, Lucas WJ** (2004) A systemic small RNA signaling system in plants. Plant Cell **16:** 1979–2000

**Zhang Y** (2005) miRU: an automated plant miRNA target prediction server. Nucleic Acids Res **33:** W701–W714